Advanced Research in Electrical and Electronic Engineering
Print ISSN: 2349-5804; Online ISSN: 2349-5812 Volume 2, Number 6 April-June (2015) pp. 52-56

http://www.krishisanskriti.org/areee.html

Naturally Clamped Soft-Switching Current- Fed Push-Pull DC/DC Converter for Fuel-Cell Application

Bharath Kumar K[1] and Shankaralingappa C B[2]

[1]4th Sem M.Tech, Dr. Ambedkar Institute of Technology, Karnataka, Bangalore-560056
[2]Dr. Ambedkar Institute of Technology, Karnataka, Bangalore-560056
E-mail: [1]bharathkumarmagi@gmail.com

Abstract—*The Present situstion wherein the transportation mainly depends on the fossil fuel extracts is really a concern since they may soon become extinct and at the same time pollution may become intolerable. So Environment friendly propulsion system are gaining popularity whwerein fuel cells come into picture. The voltage generated by fuel cells are not quiet sufficient dc-dc converters are to be designed.*
This project focuses on an external snubberless, pushpull dc-dc converter with zero voltage and zero current switching features for interfacing a low-voltage dc bus with a high voltage bus, suitable for fuel cell applications.

Index Terms*: Bidirectional converter, current-fed dc-dc converter, fuel cell vehicle(FCV), high frequency, soft switching*

1. INTRODUCTION

TRANSPORTATION electrification has received significant interest owing to limited supply of fossil fuels and concern of global climate change [1-2]. Battery based Electric vehicles (EVs) and Fuel Cell Vehicles (FCVs) are emerging as viable solutions for transportation electrification with lower emission, better vehicle performance and higher fuel economy. Compared with pure battery based EVs, FCVs are quite appealing with the merits of zero-emission, satisfied driving range, short refueling time, high efficiency, and high reliability. A diagram of a typical FCV propulsion system is shown in Fig. 1 [3-5]. Bidirectional and unidirectional dc/dc converters are utilized to develop high voltage bus for the inverter. The energy storage system (ESS) is used to overcome the limitations of lacking energy storage capability and fast power transient of FCVs.

The DC-DC converter used is push pull converter. Push pull converter has only two devices on the primary side of the frequency transformer leading to simple and reduced gating requirements.

1. The basic push-pull converter used in proposed work has the advantages:

2. A single devicevoltage drop on the input side, Where the source dc voltage is low(12V to 24V) and the current may be high.

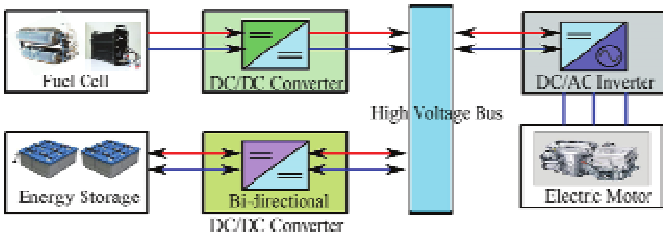

Fig. 1: Diagram of a FCV propulsion system.

3.. Zero voltage turn-on of switching devices due to commutation of the transformer magnetizing current. With paralleled MOSFET switches, zero voltage turn-off is provided by the inherent drain-source capacitance of the switches.

switch voltage ratings enabling the use of switches with low on-state resistance. This can significantly reduce conduction loss of primary side switches. However, voltage-fed converters suffer from several limitations, i.e. high pulsating current at input, limited soft-switching range, rectifier diode ringing, duty cycle loss (if inductive output filter), high circulating current through devices and magnetics, and relatively low efficiency for high voltage amplification and high input current applications. Compared with voltage-fed converters, current-fed converters exhibit smaller input current ripple, lower diode voltage rating, lower transformer turns-ratio, negligible diode ringing, no duty cycle loss, and easier current control ability low. Besides, current-fed converters can precisely control the charging and discharging current of ESS, which helps achieving higher charging/discharging efficiency. Thus current-fed converter is more feasible for the application of ESS in FCVs.

Three topologies of isolated current-fed dc/dc converters, i.e. full-bridge [10-12], L-type half bridge [13-15], and push-pull [16-17] have been researched. One drawback of current-fed converters is the high turn -off voltage spike across the devices. Normally, active -clamp circuits [14-16, 24-25], RCD passive snubbers [11] or energy recovery snubber [6] are employed to absorb the surge voltage and assist soft-switching. In RCD snubbers, energy absorbed by the clamping capacitor is dissipated in the resistor resulting in low efficiency. Active-clamp suffers from high current stress (peak) and higher circulating current at light load.

The leakage inductance and parasitic capacitance of the HF transformer were utilized to achieve zero current switching (ZCS) in [17-19]. However, resonant current is much higher than input current that increases the current stress of devices and magnetics requiring higher VA rating components. 2

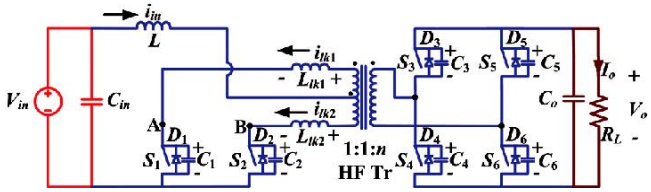

Fig. 2: Proposed ZCS current-fed push-pull dc/dc converter.

can be recycled, the auxiliary circuits still contribute to a significant amount of loss. In current-fed bidirectional converter, active soft commutation technique [11, 29-30] is proposed to divert the switch current to another switch through transformer to achieve natural or zero current commutation thus reducing or eliminating the need of snubber.

In this paper, a novel secondary modulation based naturally clamped soft-switching bidirectional snubberless current-fed push-pull converter is proposed as shown in Fig. 2. Natural voltage clamping (NVC) with ZCS of primary devices is achieved by proposed secondary modulation and therefore avoids the need of passive snubbers or active-clamp making it snubberless. Switching losses are reduced significantly owing to ZCS of primary switches and ZVS of secondary switches that permits HF switching operation with smaller magnetics.

The objectives of this paper are to explain steady-state operation and analysis, illustrate design, and demonstrate experimental performance of the proposed converter. The objectives are realized and outlined in various Sections as follows: Steady-state operation of the converter is explained and its mathematical analysis is reported in Section II. Detailed converter design procedure is illustrated in Section III. Analysis and design are verified by simulation results using PSIM 9.0.4 in Section IV. Experimental results on a laboratory prototype of 250W are demonstrated to validate and show the converter performance in Section IV.

2. OPERATION AND ANALYSIS OF THE CONVERTER

For the sake of simplicity, the following assumptions are made to study the operation and explain the analysis of the converter: a) Boost inductor L is large enough to maintain constant current through it. b) All the components are ideal. c) Series inductors L_{lk1} and L_{lk2} include the leakage inductances of the transformer. The total value of L_{lk1} and L_{lk2} is represented as L_{lk_T}. L_{lk} represents the equivalent series inductor reflected to the high voltage side. d) Magnetizing inductance of the transformer is infinitely large.

A. Boost mode (Discharging Mode) Operation

In this part, steady-state operation and analysis with zero current commutation (ZCC) and NVC concept has been explained. Before turning off one of primary side switches (say S_1), the other switch (say S_2) is turned-on. Reflected output voltage $2Vo/n$ appears across the transformer primary. It diverts the current from one switch to the other one through transformer causing current through just triggered switch to rise and the current through conducting switch to fall to zero naturally resulting in ZCC. Later the body diode across switch start conducting and its gating signal is removed leading to ZCS turn-off of the device. Commutated device capacitance starts charging with NVC.

The steady-state operating waveforms of boost mode are shown in Fig. 3. The primary switches S_1 and S_2 are operated with identical gating signals phase -shifted with each other by 180^o with an overlap. The overlap varies with duty cycle, and the duty cycle should be kept above 50%. The steady-state operation of the converter during different intervals in a one half HF cycle is explained using the equivalent circuits shown in Fig. 4. For the rest half cycle, the intervals are repeated in the same sequence with other symmetrical devices conducting to complete the full HF cycle.

Interval 1 (Fig. 4a; $t_o < t < t_1$): In this interval, primary side switches S_2 and anti-parallel body diodes D_3 and D_6 of secondary side H-bridge switches are conducting. Power is transferred to the load through HF transformer. The non-conducting secondary devices S_4 and S_5 are blocking output voltage V_o and the non-conducting primary devices S_1 is blocking reflected output voltage $2V_o/n$. The values of current through various components are:

i_{S1} =0, i_{S2} =I_{in} , i_{lk1}=0, i_{lk2}= I_{in}, i_{D3} = i_{D6}= I_{in}/n. Voltage across the switch S_1: $V_{S1} = 2V_o/n$.

Voltage across the switches S_4 and S_5: V_{S4} =V_{S5} = V_o.

Interval 2 (Fig. 4b; $t_1 < t < t_2$): At $t = t_1$, primary switch S_1 is turned-on. The corresponding snubber capacitor C_1 discharges in a very short period of time.

Interval 3 (Fig. 4c; $t_2 < t < t_3$): All two primary switches are conducting. Reflected output voltages appear across inductors L_{lk1} and L_{lk2}, diverting/transferring the current through switch S_2 to S_1. It causes current through previously conducting device S_2 to reduce linearly. It also results in conduction of switch S_1 with zero current which helps reducing associated turn- on loss. The currents through various components are given by

$$i_{lk1} i_{S1} \quad \frac{2V_o}{n L_{lk\_T}} (t \quad t_2) \tag{1}$$

$$i_{lk2} i_{S2} \quad I_{in} \quad \frac{2V_o}{n L_{lk\_T}} (t\ t_2) \tag{2}$$

$$I_{in} \quad \frac{4V_o}{} (t\ t_2)$$

$$i_{D3}\ i_{D6} \quad n \quad n^2 L$$

$$\bar{lkT} \tag{3}$$

Where $L_{lk\_T} = L_{lk1}+L_{lk2}$. At the end of this interval $t=t_3$, the anti-parallel body diode D_3 and D_6 are conducting. Therefore S_3 and S_6 can be gated on for ZVS turn-on. At the end of this interval, D_3 and D_6 commutates naturally. Current through all primary devices reaches $I_{in}/2$. Final values are: $i_{lk1} = i_{lk2} = I_{in}/2$, $i_{S1} = i_{S2} = I_{in}/2$, $i_{D3} = i_{D6} = 0$.

Interval 4 (Fig. 4d; $t_3 < t < t_4$): In this interval, secondary H-bridge devices S_3 and S_6 are turned-on with ZVS. Currents through all the switching devices continue increasing or decreasing with the same slope as interval 3. At the end of this interval, the primary device S_2 commutates naturally with ZCC and the respective current i_{S2} reaches zero obtaining ZCS. The full current, i.e. input current is taken over by other device S_1.

Final values are: $i_{lk1} = i_{S1} = I_{in}$, $i_{lk2} = i_{S2} = 0$, $i_{S3} = i_{S6} = I_{in}/n$.

Interval 5 (Fig. 4e; $t_4 < t < t_5$): In this interval, the leakage inductance current i_{lk1} increases further with the same slope and anti-parallel body diode D_2 starts conducting causing extended zero voltage to appear across commutated switch S_2 to ensure ZCS turn- off. Now, the secondary devices S_3 and S_6 are turned-off. At the end of this interval, current through switch S_1 reaches its peak value. This interval should be very short to limit the peak current though the transformer and switch reducing the current stress and kVA ratings.

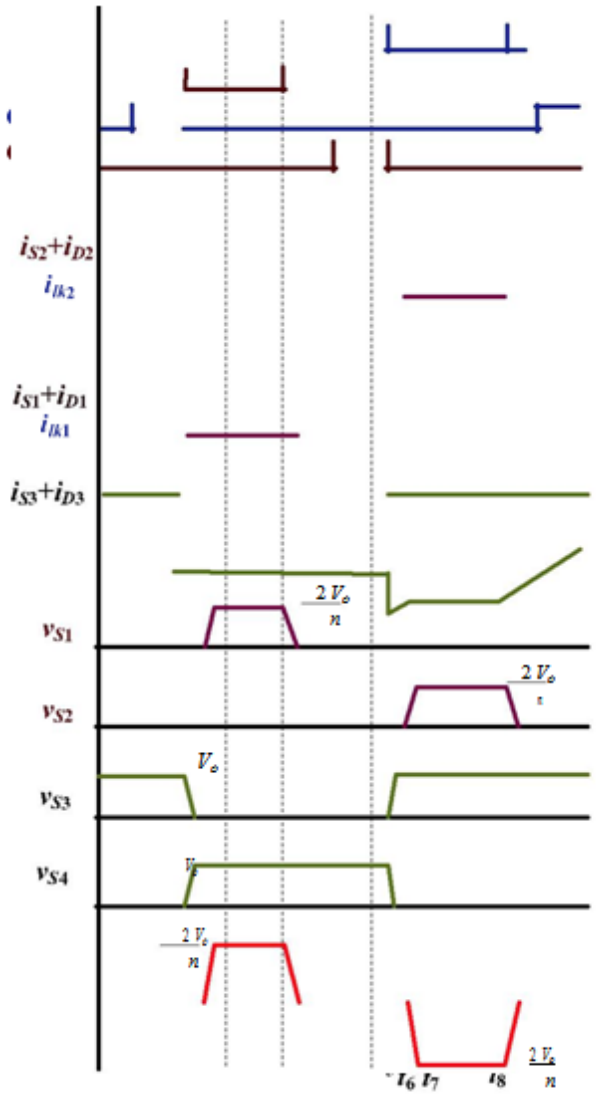

Fig. 3: Operating waveforms of proposed ZCS current-fed push-pull converter in the boost mode.

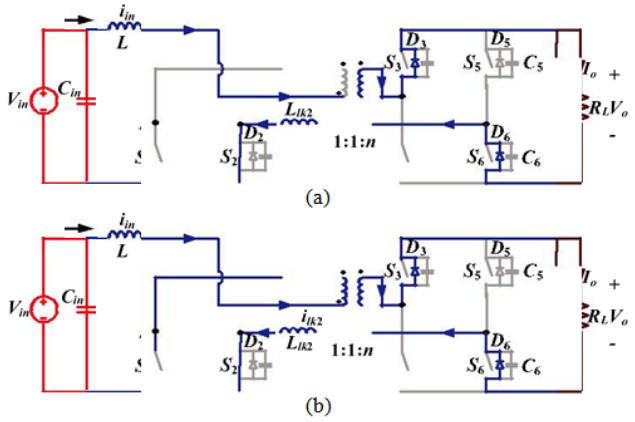

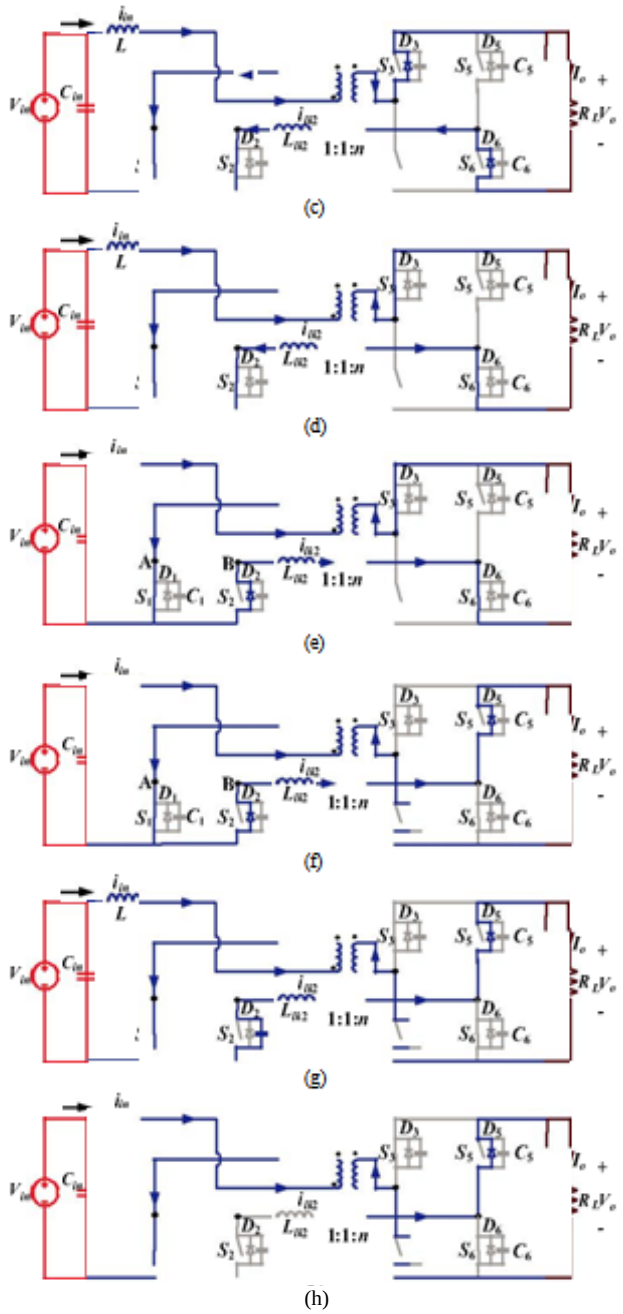

Fig. 4: Equivalent circuits during different intervals of the boost mode operation.

The currents through operating components are given by

$$i_{S1} = i_{lk1} = i_{in} - \frac{2V_o}{nL_{lk\_T}}(t - t_4) \quad (4)$$

$$i_{D2} = i_{lk2} = \frac{2V_o}{nL_{lk\_T}}(t - t_4) \quad (5)$$

$$i_{S3} = i_{S6} = \frac{i_{in}}{n} - \frac{4V_o}{n^2 L_{lk\_T}}(t - t_4) \quad (6)$$

Interval 6 (Fig. 4f; $t_5 < t < t_6$): During this interval, secondary switches S_3 and S_6 are turned-off. Anti-parallel body diodes of switches S_4 and S_5 take over the current immediately. Therefore, the voltage across the transformer primary reverses turn-off of the primary switches and ZVS turn- on of the secondary side switches mentioned above, the total switching losses are reduced enormously.

Voltages across the primary winding of the HF transformer V_{AB} are illustrated in parts (b) of Figs. 10-11. The high-frequency bipolar voltage waveform clearly states the clamped devices' voltage (less than 100V). Low on-state resistance can be used due to the naturally low clamped voltage across them resulting in lower conduction loss and higher efficiency. Parts (a) of Figs. 12-13 show the boost inductor current waveforms with 2x device switching frequency, which brings a reduction of size of the inductor.

Fig. 12 shows measured efficiency for different load for the proposed design and the developed laboratory prototype. The peak efficiency of 93.6% for 200W and full load efficiency 92.9% for 250W are obtained in forward direction.

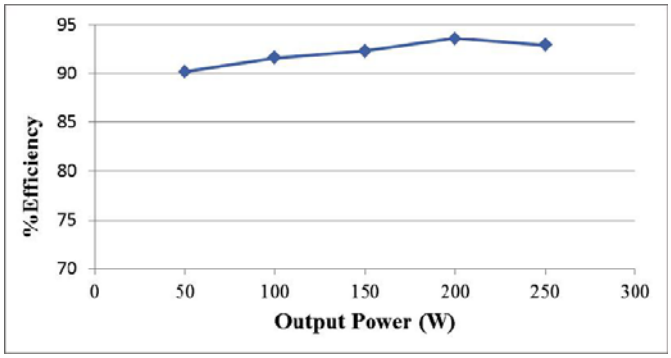

Fig. 12: Plot of efficiency versus output power for different load condition.

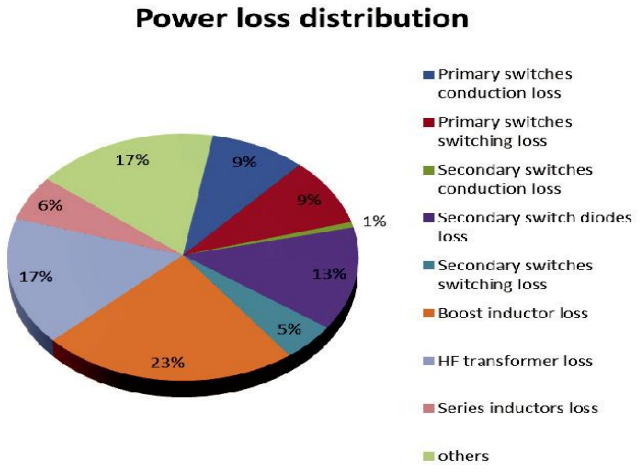

Fig. 13: Loss comparison of proposed converter at full load condition.

Loss distribution estimation from the loss model given in [31] is Fig. 13. It is easy to find that conduction losses of primary devices are rather low because of the usage of low voltage devices. Switching loss of both sides of HF transformer are reduced significantly due to soft switching. A considerable part of total loss is from boost inductor and HF transformer. The percentage of this part of loss can be reduced with the increase of power level and optimized design. Compared with similar topologies with active-clamp circuits or snubber circuits, efficiency can be improved more than 2% for the experimental prototype.

3. SUMMARY AND CONCLUSIONS

This paper presents a novel soft-switching snubberless bidirectional current-fed isolated push- pull dc/dc converter for application of the ESS in FCVs. A novel secondary side modulation method is proposed to eliminate the problem of oltage spike across the semiconductor devices at turn-off. The above claimed ZCC and NVC of primary devices without any snubber are demonstrated and confirmed by the simulation and experimental results. ZCS of primary side devices and ZVS of secondary side devices are achieved, which reduces the switching losses significantly. Soft- switching is inherent and is maintained independent of load. Once ZCC, NVC, and soft-switching are designed to be obtained at rated power, it is guaranteed to happen at reduced load unlike voltage-fed converters. Turn-on switching transition loss of primary devices is also shown to be negligible. Hence maintaining soft-switching of all devices substantially reduces the switching loss and allows higher switching frequency operation for the converter to achieve a more compact and higher power density system. Proposed secondary modulation achieves natural commutation of primary devices and clamps the voltage across them at low voltage (reflected output voltage) independent of duty cycle. It therefore eliminates requirement of active-clamp or passive nubber. Usage of low voltage devices results in low conduction losses in primary devices, which is significant due to higher currents on primary side. The proposed modulation method is simple and easy to implement. These merits make the converter promising for interfacing low voltage dc bus with high voltage dc bus for higher current applications such as FCVs, front-end dc/dc power conversion for renewable (fuel cells/PV) inverters, UPS, microgrid, V2G, and energy storage. The specifications are taken for FCV but the proposed modulation, design, and the demonstrated results are suitable for any general application of current-fed converter (high step-up). Similar merits and performance will be achieved.

REFERENCES

[1] A. Khaligh and Z. Li, “Battery, ultracapacitor, fuel cell, and hybrid energy storage systems for electric, hybrid electric, fuel cell, and plug-in hybrid electric vehicles: State of the art”, *IEEE Trans. on Vehicular Technology*, vol. 59, no. 6, pp. 2806- 2814, Oct. 2009.

[2] A. Emadi, and S. S. Williamson, “Fuel cell vehicles: opportunities and challenges,” in *Proc. IEEE PES*, 2004, pp. 1640-1645.

[3] K. Rajashekhara, “Power conversion and control strategies for fuel cell vehicles,” in *Proc. IEEE IECON*, 2003, pp. 2865-2870.

[4] A. Emadi, S. S. Williamson, and A. Khaligh, “Power electronics intensive solutions for advanced electric, hybrid electric, and fuel cell vehicular power systems,” *IEEE Trans. Power Electron.*, vol. 21, no. 3, pp. 567–577, May. 2006.

[5] A. Emadi, K. Rajashekara, S. S. Williamson, and S. M. Lukic, “Topological overview of hybrid electric and fuel cell vehicular power system architectures and configurations” *IEEE Trans. on Vehicular* Technology, vol. 54, no. 3, pp. 763–770, May. 2005.

[6] T.-F. Wu, Y.-C. Chen, J.-G. Yang, and C.-L. Kuo, “Isolated bidirectional full-bridge DC–DC converter with a flyback snubber,” *IEEE Trans. Power Electron*., vol. 25, no. 7, pp. 1915–1922, Jul. 2010.

[7] Y. Kim; I. Lee; I.Cho; G. Moon, “Hybrid dual full-bridge DC–DC converter with reduced circulating current, output filter, and conduction loss of rectifier stage for RF power generator application," *IEEE Trans. Power Electron.*, vol.29, no.3,